

Terminal Aminophosphinidene Complexes of Iron, Ruthenium, and Osmium

Brian T. Sterenberg,[†] Konstantin A. Udachin, and Arthur J. Carty*

Steacie Institute for Molecular Sciences, National Research Council Canada, 100 Sussex Drive, Ottawa, Ontario, Canada K1A 0R6, and the Ottawa-Carleton Chemistry Research Institute, Department of Chemistry, University of Ottawa, Ottawa, Ontario, Canada K1N 6N5

Received May 27, 2003

The chloroaminophosphido complexes $[\text{Cp}^*\text{M}(\text{CO})_2\{\text{P}(\text{Cl})\text{N}^i\text{Pr}_2\}]$ (**1**, M = Fe; **2**, M = Ru; **3**, M = Os), formed by the reaction of $[\text{Cp}^*\text{M}(\text{CO})_2]^-$ with $^i\text{Pr}_2\text{NPCI}_2$, undergo abstraction of chloride by aluminum trichloride, affording isolable, thermally stable, cationic terminal aminophosphinidene complexes $[\text{Cp}^*\text{M}(\text{CO})_2\{\text{PN}^i\text{Pr}_2\}][\text{AlCl}_4]$ (**4**, M = Fe; **5**, M = Ru; **6**, M = Os). The structures of all three complexes have been determined by single-crystal X-ray diffraction. The iron complex **4** has historical significance, having been spectroscopically detected at low temperature in 1984, prior to the description of the first stable η^1 -phosphinidene complex, but not isolated or structurally characterized.

Introduction

Stable, terminal phosphinidene complexes were first described by Lappert in 1987.¹ Like carbenes, terminal phosphinidene complexes can be roughly divided into electrophilic or nucleophilic categories on the basis of their reactivities.² For many years, the only stable terminal phosphinidene complexes were nucleophilic phosphinidene complexes of early transition metals.³ Electrophilic phosphinidene complexes have however been extensively studied as transient species.⁴ In 2001, we reported the successful isolation of the first amino-phosphinidene complexes and presented examples of molybdenum and tungsten η^1 -phosphinidenes, as well as the first stable late metal phosphinidene compound, a complex of ruthenium.⁵ Like the heteroatom substitu-

ent of a Fischer carbene complex, the amino group on the phosphinidene forms a donor interaction with the phosphorus atom, stabilizing the electrophilic center.

Since that report, there has been greatly increased interest in the synthesis of terminal late metal phosphinidene complexes, and examples of nickel,⁶ iridium,^{7,8} rhodium,⁸ and cobalt^{8,9} complexes have recently been reported, including examples with heteroatom substituents and bulky aryl substituents. In the specific context of this paper, the first neutral η^6 -arene ruthenium and osmium complexes $[(\eta^6\text{-Ar})(\text{L})\text{M}=\text{PMes}^*]$ bearing terminal, bulky phosphinidene ligands have recently been described.¹⁰ Although steric encumbrance around the phosphorus atom has often been considered necessary to stabilize these compounds, the isolation and characterization of a cobalt complex $[\text{Co}(\text{CO})_3(\text{PPh}_3)(\eta^1\text{-PN}^i\text{Pr}_2)][\text{AlCl}_4]$ lacking steric protection suggest that electronic stabilization of the phosphinidene is important. By analogy with carbenes, late metal phosphinidene complexes can be expected to have properties intermediate between electrophilic and nucleophilic phosphinidene complexes.

This full paper follows our communication on the ruthenium complex **4** and reports the synthesis and characterization of cationic phosphinidene complexes of the entire triad of Fe, Ru, and Os group 8 metals, including the first stable terminal phosphinidene of iron. We also describe the chloroaminophosphido complexes, which serve as precursors to the phosphinidene complexes.

* Corresponding author. E-mail: arthur.carty@nrc.ca. Tel: (613) 993 2024. Fax: (613) 957 8850.

[†] Current address: Department of Chemistry and Biochemistry, University of Regina, 3737 Wascana Parkway, Regina, Saskatchewan, S4S 0A2, Canada.

(1) Hitchcock, P. B.; Lappert, M. F.; Leung, W.-P. *J. Chem. Soc., Chem. Commun.* **1987**, 1282.

(2) Ehlers, A. W.; Baerends, E. J.; Lammertsma, K. *J. Am. Chem. Soc.* **2002**, *124*, 2831. Frison, G.; Mathey, F.; Sevin, A. *J. Organomet. Chem.* **1998**, *570*, 225. Creve, S.; Pierloot, K.; Nguyen, M. T.; Vanquickenborne, L. G. *Eur. J. Inorg. Chem.* **1999**, 107. Ehlers, A. W.; Lammertsma, K.; Baerends, E. J. *Organometallics* **1998**, *17*, 2738.

(3) Dillon, K. B.; Mathey, F.; Nixon, J. F. *Phosphorus: The Carbon Copy*; John Wiley & Sons: Ltd.: Chichester, 1998.

(4) Sava, X.; Marinetti, A.; Ricard, L.; Mathey, F. *Eur. J. Inorg. Chem.* **2002**, 2002, 1657. Tran Huy, N. H.; Compain, C.; Ricard, L.; Mathey, F. *J. Organomet. Chem.* **2002**, *650*, 57. Vlaar, M. J. M.; Valkier, P.; Schakel, M.; Ehlers, A. W.; Lutz, M.; Spek, A. L.; Lammertsma, K. *Eur. J. Org. Chem.* **2002**, 1797. Vlaar, M. J. M.; van Assema, S. G. A.; de Kanter, F. J. J.; Schakel, M.; Spek, A. L.; Lutz, M.; Lammertsma, K. *Chem. Eur. J.* **2002**, *8*, 58. Tran Huy, N. H.; Ricard, L.; Mathey, F. *New J. Chem.* **1998**, 75. Vlaar, J. M.; de Kanter, F. J. J.; Schakel, M.; Lutz, M.; Spek, A. L.; Lammertsma, K. *J. Organomet. Chem.* **2001**, *617–618*, 311. Tran Huy, N. H.; Ricard, L.; Mathey, F. *J. Organomet. Chem.* **1999**, *582*, 53. Wit, J. B. M.; van Eijkel, G. T.; de Kanter, F. J. J.; Schakel, M.; Ehlers, A. W.; Lutz, M.; Spek, A. L.; Lammertsma, K. *Angew. Chem., Int. Ed.* **1999**, *38*, 2596. Tran Huy, N. H.; Mathey, F. *J. Org. Chem.* **2000**, *65*, 652. Mathey, F.; Tran Huy, N. H.; Marinetti, A. *Helv. Chim. Acta* **2001**, *84*, 2938. Lammertsma, K.; Vlaar, M. J. M. *Eur. J. Org. Chem.* **2002**, 1127.

(5) Sterenberg, B. T.; Udachin, K. A.; Carty, A. J. *Organometallics* **2001**, *20*, 2657.

(6) Melenkivitz, R.; Mindiola, D. J.; Hillhouse, G. L. *J. Am. Chem. Soc.* **2002**, *124*, 3846.

(7) Termaten, A. T.; Nijbacker, T.; Schakel, M.; Lutz, M.; Spek, A. L.; Lammertsma, K. *Organometallics* **2002**, *21*, 3196.

(8) Termaten, A. T.; Aktas, H.; Schakel, M.; Ehlers, A. W.; Lutz, M.; Spek, A. L.; Lammertsma, K. *Organometallics* **2003**, *22*, 1827.

(9) Sánchez-Nieves, J.; Sterenberg, B. T.; Udachin, K. A.; Carty, A. J. *J. Am. Chem. Soc.* **2003**, *125*, 2404.

(10) Termaten, A. T.; Nijbacker, T.; Schakel, M.; Lutz, M.; Spek, A. L.; Lammertsma, K. *Chem. Eur. J.* **2003**, *9*, 2200.

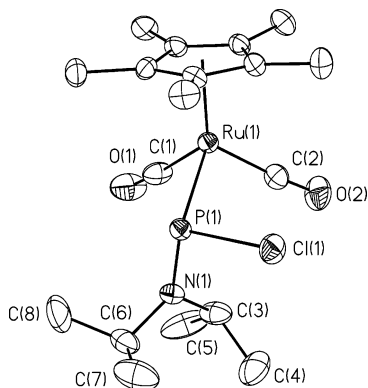


Figure 1. ORTEP diagram of $[\text{Cp}^*\text{Ru}(\text{CO})_2\{\text{P}(\text{Cl})\text{N}^i\text{Pr}_2\}]$ (**2**). Thermal ellipsoids are shown at the 50% level, and hydrogen atoms have been eliminated for clarity.

Scheme 1

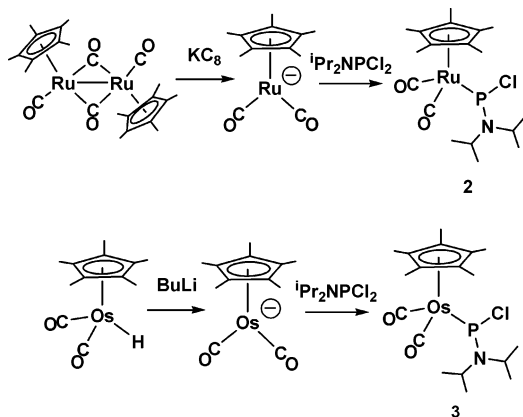


Table 1. Selected Distances and Angles for $[\text{Cp}^*\text{Ru}(\text{CO})_2\{\text{P}(\text{Cl})\text{N}^i\text{Pr}_2\}]$ (**2**)

Ru(1)–C(2)	1.873(5)	C(1)–Ru(1)–P(1)	88.3(2)
Ru(1)–C(1)	1.888(4)	N(1)–P(1)–Cl(1)	102.7(1)
Ru(1)–P(1)	2.373(1)	N(1)–P(1)–Ru(1)	114.2(1)
Cl(1)–P(1)	2.213(1)	Cl(1)–P(1)–Ru(1)	102.01(5)
P(1)–N(1)	1.682(4)	C(3)–N(1)–C(6)	115.9(4)
O(1)–C(1)	1.124(6)	C(3)–N(1)–P(1)	124.6(3)
O(2)–C(2)	1.152(6)	C(6)–N(1)–P(1)	117.4(3)
C(2)–Ru(1)–C(1)	94.9(2)	O(1)–C(1)–Ru(1)	175.4(5)
C(2)–Ru(1)–P(1)	96.4(1)	O(2)–C(2)–Ru(1)	175.6(4)

Results and Discussion

Formation of Phosphido Complexes. The precursors we have used to access terminal phosphinidene complexes are the terminal chloroaminophosphido complexes $[\text{Cp}^*\text{M}(\text{CO})_2\{\text{P}(\text{Cl})\text{N}^i\text{Pr}_2\}]$ (**1**, $\text{M} = \text{Fe}$; **2**, $\text{M} = \text{Ru}$; **3**, $\text{M} = \text{Os}$). The Fe complex has been previously prepared but not structurally characterized,¹¹ and the ruthenium and osmium complexes were formed by reacting the appropriate $\text{Cp}^*\text{M}(\text{CO})_2^-$ anion with $\text{Cl}_2\text{-PN}^i\text{Pr}_2$ as shown in Scheme 1.

To provide structural details for this series of terminal phosphido compounds, we carried out a single-crystal X-ray study of the ruthenium complex. An ORTEP diagram is shown in Figure 1, and selected bond distances and angles are given in Table 1. The geometry at the ruthenium atom is that of a three-legged piano stool, with two carbonyl ligands and the phosphido group forming the legs of the stool. The Ru–P distance

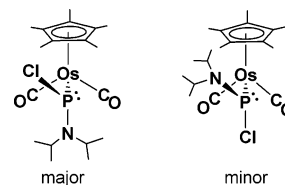


Figure 2. Isomers of $[\text{Cp}^*\text{Os}(\text{CO})_2\{\text{P}(\text{Cl})\text{N}^i\text{Pr}_2\}]$ (**3**).

of 2.373(1) Å is consistent with a Ru–P single bond. For comparison, the ruthenium–phosphorus bond distance in the related phosphido complex $[\text{Cp}^*\text{Ru}(\text{CO})_2\{\text{P}(\text{C}(\text{O})^t\text{Bu})_2\}]$ is 2.404(1) Å,¹² while the distance in the cationic phosphine complex $[\text{Cp}^*\text{Ru}(\text{CO})_2\text{PPh}_3]^+$ is 2.361–(2) Å.¹³ The geometry at phosphorus is pyramidal, indicating that there is a stereoactive lone pair and that the phosphido ligand is acting as a one-electron donor. Along with the Cp* ring and two carbonyls, the one-electron-donor phosphido group results in an 18-electron configuration at the Ru(II) center.

The conformation at the phosphorus atom is such that the isopropylamino group is directed away from the Cp* ring, while the chlorine atom and the lone pair point toward the ring. The P–N distance of 1.682(4) Å is typical for a PN single bond (cf. 1.678(26) Å average in aminophosphines¹⁴). The geometry at nitrogen is slightly pyramidal, with the N atom deviating by 0.1272 Å from the plane defined by the phosphorus and two carbon atoms C(3) and C(6).

The compounds each show singlets in the ³¹P NMR spectrum at δ 346 (Fe),¹¹ 341 (Ru), and 304 (Os). This shift to higher field of ³¹P resonances as the triad is descended is commonly observed for isostructural compounds and has been attributed to increased shielding by the heavier metals.¹⁵ The solution infrared spectra of **1** and **2** show two carbonyl bands as expected, while the osmium analogue **3** shows four carbonyl bands, indicating the presence of a major and a minor isomer in solution, attributed to two conformations of the phosphido ligand as illustrated in Figure 2. The observation of two conformers in the osmium complex probably results from the longer Os–P bond. In the Ru and Fe complexes, the minor isomer is more sterically hindered due to interaction of the isopropyl groups with the Cp* ring and isomerism is not observed.

At room temperature, the ¹H NMR spectra of the phosphido complexes show broad peaks for the isopropyl CH and CH₃ groups. The ruthenium complex was studied by variable-temperature NMR spectroscopy. The low-temperature limiting spectrum (–60 °C) shows two CH groups (apparent septets) and four methyl groups (doublets). At this temperature, the two isopropyl groups are inequivalent, indicating that there is a barrier to rotation about the PN bond, and the methyl groups are diastereotopic as a result of the stereogenic phosphorus center. As the temperature is increased, several changes occur. First, the two pairs of methyl resonances coalesce

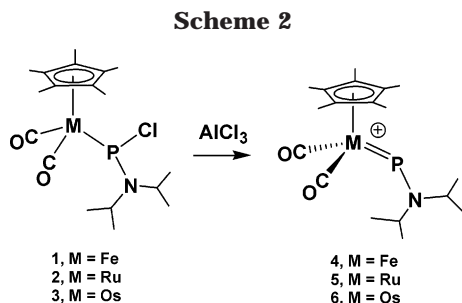
(12) Weber, L.; Reizig, K.; Boese, R. *Organometallics* **1985**, *4*, 1890. Weber, L.; Bungardt, D.; Reizig, K.; Boese, R. *Z. Naturforsch., Teil B* **1986**, *41*, 1096.

(13) Bruce, M. I.; Zaitseva, N. N.; Skelton, B. W.; White, A. H. *Aust J. Chem.* **1998**, *51*, 433–435.

(14) Orpen, A. G.; Brammer, L.; Allen, F. H.; Kennard, O.; Watson, D. G.; Taylor, R. *J. Chem. Soc., Dalton Trans.* **1989**, S1.

(15) Carty, A. J.; MacLaughlin, S. A.; Nucciarone, D. In *Phosphorus-31 NMR Spectroscopy in Stereochemical Analysis*; Verkade, J. G., Quin, L. D., Eds.; VCH: Deerfield Beach, 1987; pp 559–619.

(11) Nakazawa, H.; Buhro, W. E.; Bertrand, G.; Gladysz, J. A. *Inorg. Chem.* **1984**, *23*, 3431.



into two broad peaks. This corresponds to inversion at phosphorus. Coalescence temperatures for each pair are estimated to be -40 and -10 °C, allowing a rough calculation of 11.9 ± 0.5 kcal/mol as the barrier to inversion at phosphorus. Further increase in temperature leads to coalescence of the two remaining methyl resonances ($+15$ °C) and the CH resonances ($+32$ °), resulting from rotation about the PN bond. The barrier to inversion for this process is estimated as 14.1 ± 0.5 kcal/mol. In the related molybdenum system $[\text{Cp}^*\text{Mo}(\text{CO})_3\{\text{P}(\text{Cl})\text{N}^i\text{Pr}_2\}]$, the barrier to PN rotation was comparable at 15 kcal/mol, but the barrier to inversion at phosphorus was substantially greater at over 17 kcal/mol.¹⁶ Reported barriers to inversion at phosphorus in metal phosphido complexes range from 11.5 to 18.0 kcal/mol.¹⁷

Chloride Abstraction and Formation of Phosphinidene Complexes. Abstraction of chloride ion from $[\text{Cp}^*\text{Fe}(\text{CO})_2\{\text{P}(\text{Cl})\text{N}^i\text{Pr}_2\}]$ (**1**) with an excess of AlCl_3 in dichloromethane leads to the phosphinidene complex $[\text{Cp}^*\text{Fe}(\text{CO})_2\{\text{PN}^i\text{Pr}_2\}][\text{AlCl}_4]$ (**4**) (Scheme 2). The synthesis of **4** was initially attempted by Gladysz and co-workers in 1984,¹¹ well before the characterization of the first stable terminal phosphinidene complex by Lappert.¹ Halide abstraction from the iron phosphido complex $[\text{Cp}^*\text{Fe}(\text{CO})_2\{\text{P}(\text{Cl})\text{N}^i\text{Pr}_2\}]$ (**1**) with $[\text{Ph}_3\text{C}][\text{PF}_6]$ or AlCl_3 led to the observation by ^{31}P NMR at -90 °C of a thermally unstable complex tentatively identified as $[\text{Cp}^*\text{Fe}(\text{CO})_2\{\text{PN}^i\text{Pr}_2\}]^+$. This compound is in fact thermally stable in the absence of water. Rigorously anhydrous conditions are necessary to successfully form **4**, as it is extremely sensitive to water, and an excess of AlCl_3 helps to remove the last traces of water from the solvent.

The room-temperature ^{31}P NMR spectrum of **4** shows a peak at δ 965. This chemical shift differs somewhat from the value of δ 954 reported by Gladysz et al.; however, that value was recorded at -90 °C. At -90 °C we also observe a chemical shift of δ 954. The ^1H NMR spectrum of **4** shows peaks for two inequivalent isopropyl groups, indicating that there is a barrier to rotation about the PN bond. No exchange between the isopropyl groups is observed even at elevated temperatures. The two methyl groups of each isopropyl group are equivalent as a result of the symmetry plane that contains iron, phosphorus, nitrogen, and the central carbon of each isopropyl group.

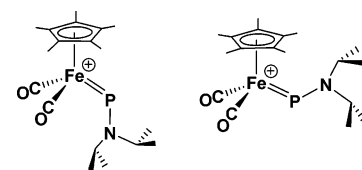


Figure 3. Isomers of $[\text{Cp}^*\text{Fe}(\text{CO})_2\{\text{PN}^i\text{Pr}_2\}]^+$ (**4**).

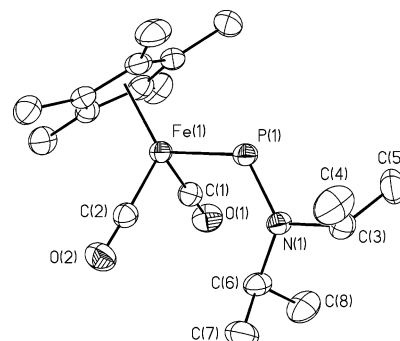


Figure 4. ORTEP diagram of the cation of $[\text{Cp}^*\text{Fe}(\text{CO})_2\{\text{PN}^i\text{Pr}_2\}][\text{AlCl}_4]$ (**4**). Thermal ellipsoids are shown at the 50% level, and hydrogen atoms have been eliminated for clarity.

Table 2. Selected Distances and Angles for $[\text{Cp}^*\text{Fe}(\text{CO})_2\{\text{PN}^i\text{Pr}_2\}][\text{AlCl}_4]$ (**4**)

molecule 1		molecule 2	
Fe(1)–P(1)	2.1515(6)	Fe(2)–P(2)	2.1505(7)
P(1)–N(1)	1.629(2)	P(2)–N(2)	1.630(2)
Fe(1)–C(1)	1.782(2)	Fe(2)–C(21)	1.788(2)
Fe(1)–C(2)	1.783(2)	Fe(2)–C(22)	1.785(2)
O(1)–C(1)	1.136(3)	O(21)–C(21)	1.132(3)
O(2)–C(2)	1.138(3)	O(22)–C(22)	1.136(3)
C(1)–Fe(1)–C(2)	96.1(1)	C(21)–Fe(2)–C(22)	98.1(1)
C(1)–Fe(1)–P(1)	94.14(7)	C(21)–Fe(2)–P(2)	92.86(8)
C(2)–Fe(1)–P(1)	93.72(7)	C(22)–Fe(2)–P(2)	95.31(8)
N(1)–P(1)–Fe(1)	118.66(7)	N(2)–P(2)–Fe(2)	118.58(8)
C(6)–N(1)–C(3)	114.8(2)	C(26)–N(2)–C(23)	115.2(2)
C(6)–N(1)–P(1)	128.2(1)	C(26)–N(2)–P(2)	127.8(1)
C(3)–N(1)–P(1)	117.0(1)	C(23)–N(2)–P(2)	117.0(1)
O(1)–C(1)–Fe(1)	178.5(2)	O(21)–C(21)–Fe(2)	176.5(2)
O(2)–C(2)–Fe(1)	178.1(2)	O(22)–C(22)–Fe(2)	175.8(2)

The infrared spectrum of **4** shows two sets of carbonyl bands, suggesting that two isomers exist in solution. These isomers likely result from a rotation about the metal–phosphorus bond as shown in Figure 3. The ^1H and ^{31}P NMR spectra show no evidence of more than one isomer, indicating that interconversion is fast on the NMR time scale and that rotation about the Fe–P bond is facile.

Compound **4** crystallizes readily by slow diffusion of dry hexane into saturated CH_2Cl_2 solutions and has been structurally characterized by X-ray diffraction. An ORTEP diagram of the cation is shown in Figure 4, and distances and angles are shown in Table 2. The asymmetric unit contains two crystallographically inequivalent but virtually identical molecules. The geometry at iron is that of a three-legged piano stool, with iron bound by the Cp^* ligand, two carbonyl ligands, and the phosphorus atom. The iron–phosphorus bond length is 2.151(1) Å, somewhat longer than other iron–phosphorus double bonds (2.084–2.117 Å),¹⁸ but shorter than Fe–P single bonds, which usually lie in the range 2.20–2.30 Å.¹⁴ Other than iron, phosphorus is bound only to nitrogen. The bond angle at phosphorus is 118.6(1)°, close to the ideal trigonal geometry. The P–N distance

(16) Sterenberg, B. T.; Carty, A. J. *J. Organomet. Chem.* **2001**, 617–618, 696.

(17) Wicht, D. K.; Kovacic, I.; Glueck, D. S.; Liable-Sands, L. M.; Incarvito, C. D.; Rheingold, A. L. *Organometallics* **1999**, 18, 5141. Buhro, W. E.; Gladysz, J. A. *Inorg. Chem.* **1985**, 24, 3505. Simpson, R. D.; Bergman, R. G. *Organometallics* **1992**, 11, 3980.

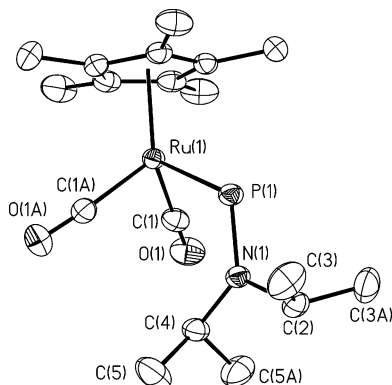


Figure 5. ORTEP diagram of the cation of $[\text{Cp}^*\text{Ru}(\text{CO})_2\{\text{PNiPr}_2\}][\text{AlCl}_4]$ (**5**). Thermal ellipsoids are shown at the 50% level, and hydrogen atoms have been eliminated for clarity.

of 1.629(4) Å is intermediate between P–N single (e.g., 1.678(26) Å average in aminophosphines) and double bonds (e.g., 1.540(22) Å average in iminophosphines).¹⁴ The amino group is directed away from the Cp* ring. The geometry at nitrogen is planar within experimental error.

We suspected that the previous failure to isolate the iron phosphinidene complex resulted from the presence of traces of water in the reaction mixture. To test this hypothesis, water was added to a sample of **2**. The ³¹P NMR spectrum showed the immediate formation of a new species with a ³¹P chemical shift of δ 121. This is the same chemical shift observed by previous workers which was attributed to the product of thermal decomposition of **2** via CH activation of the isopropyl group. What is more likely occurring, however, is either addition of water to the phosphinidene phosphorus atom, similar to the trapping reactions of transient electrophilic phosphinidene complexes with water, alcohols, or secondary amines,¹⁹ or addition of HCl formed by hydrolysis of the AlCl₄[−] anion. To test the thermal stability of **2**, a pure sample in CDCl₃ was heated to 70 °C for 1 h and showed no observable decomposition.

Chloride abstraction from the ruthenium and osmium chloroaminophosphido complexes proceeds as in the iron system, leading to $[\text{Cp}^*\text{Ru}(\text{CO})_2\{\text{PNiPr}_2\}][\text{AlCl}_4]$ (**5**) and $[\text{Cp}^*\text{Os}(\text{CO})_2\{\text{PNiPr}_2\}][\text{AlCl}_4]$ (**6**). An ORTEP diagram of the cation of complex **5** is shown in Figure 5, and selected distances and angles are shown in Table 2. The molecule lies on a crystallographic mirror plane, with Ru, P, N, C(2), C(4), C(6), and C(9), as well as Al and two Cl atoms of the counterion lying in the plane. The other atoms are symmetry pairs. The geometry at Ru is that of a three-legged piano stool. The Ru–P distance of 2.2654(5) Å is slightly shorter than typical Ru–P phosphine distances in strongly donating phosphine complexes (the average Ru–P distance in Ru–PMe₃ complexes is 2.307(50) Å). The P–N distance of 1.6273(16) Å is again intermediate between PN single and double bonds. The bond angle at phosphorus is

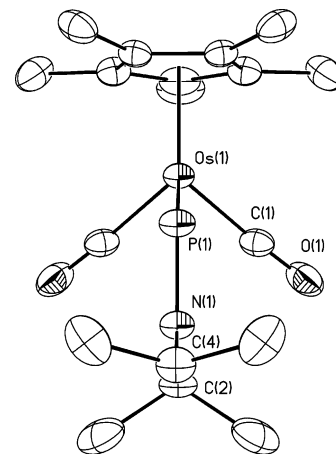


Figure 6. ORTEP diagram of the cation of $[\text{Cp}^*\text{Os}(\text{CO})_2\{\text{PNiPr}_2\}][\text{AlCl}_4]$ (**6**), viewed down the P–Os axis, emphasizing the planarity of the Os–P–N–C₂ unit. Thermal ellipsoids are shown at the 50% level, and hydrogen atoms have been eliminated for clarity.

Table 3. Selected Distances and Angles for $[\text{Cp}^*\text{Ru}(\text{CO})_2\{\text{PNiPr}_2\}][\text{AlCl}_4]$ (5**) and $[\text{Cp}^*\text{Os}(\text{CO})_2\{\text{PNiPr}_2\}][\text{AlCl}_4]$ (**6**)**

5		6	
Ru(1)–P(1)	2.2654(5)	Os(1)–C(1)	1.891(4)
P(1)–N(1)	1.627(2)	Os(1)–P(1)	2.278(2)
Ru(1)–C(1)	1.906(2)	P(1)–N(1)	1.634(5)
C(1)–O(1)	1.134(2)	O(1)–C(1)	1.152(6)
C(1)–Ru(1)–C(1)′	93.22(9)	C(1)–Os(1)–C(1)′	92.5(3)
C(1)–Ru(1)–P(1)	93.94(5)	C(1)–Os(1)–P(1)	94.2(2)
N(1)–P(1)–Ru(1)	119.58(6)	N(1)–P(1)–Os(1)	119.0(2)
C(4)–N(1)–C(2)	114.9(1)	C(2)–N(1)–C(4)	115.3(5)
C(4)–N(1)–P(1)	126.8(1)	C(2)–N(1)–P(1)	127.4(4)
C(2)–N(1)–P(1)	118.3(1)	C(4)–N(1)–P(1)	117.3(4)
O(1)–C(1)–Ru(1)	176.4(1)	O(1)–C(1)–Os(1)	176.9(4)

Table 4. Structural and Spectroscopic Features of **4, **5**, and **6****

	M	δ ³¹ P	ν(CO)	d(MP)	d(PN)
4	Fe	965	2050, 1999, 2036, 2007	2.151(1)	1.629(4)
5	Ru	932	2051, 2007	2.2654(5)	1.627(2)
6	Os	838	2055, 2005	2.278(2)	1.634(5)

119.58(6)°, close to the ideal trigonal bond angle of 120°. The Ru–P–N–C₂ unit is exactly planar, as required by the crystallographic symmetry. The X-ray structure determination shows that $[\text{Cp}^*\text{Os}(\text{CO})_2\{\text{PNiPr}_2\}][\text{AlCl}_4]$ (**6**) (Figure 6) is isomorphous and nearly identical to that of **5**.

The ³¹P{¹H} resonance for the ruthenium phosphinidene complex exhibits a typically extreme downfield shift at δ 932, while the ¹H NMR spectrum shows two inequivalent isopropyl groups. The IR spectrum of **5** shows two bands at 2051 and 2007 cm^{−1}. A direct comparison of the IR carbonyl stretching frequencies with the known compound $[(\eta^5\text{-C}_5\text{Me}_4\text{CH}_2\text{OEt})\text{Ru}(\text{CO})_2(\text{PPh}_3)]^+$ (νCO = 2054, 2005 cm^{−1}) suggests that the phosphinidene ligand has donor/acceptor properties similar to phosphines. The osmium phosphinidene complex shows similar spectroscopic properties, with a ³¹P chemical shift of δ 838 and IR carbonyl bands at 2055 and 2005 cm^{−1}.

The important structural and spectroscopic features of the three phosphinidene complexes are shown in Table 3. The ³¹P chemical shifts vary as expected, with the iron complex displaying the lowest field chemical

(18) Weber, L.; Buchwald, S.; Lentz, D.; Preugschat, D.; Stammler, H. G.; Neumann, B. *Organometallics* **1992**, *11*, 2351. Weber, L.; Frebel, M.; Boese, R. *New J. Chem.* **1989**, *13*, 303. Cowley, A. H.; Kemp, R. A.; Ebsworth, E. A. V.; Rankin, D. W. H.; Walkinshaw, M. D. *J. Organomet. Chem.* **1984**, *265*, C19.

(19) Mathey, F. *Angew. Chem., Int. Ed. Engl.* **1987**, *26*, 275. Marinetti, A.; Mathey, F. *J. Am. Chem. Soc.* **1982**, *104*, 4484.

Table 5. Crystal Data for Compounds 2 and 4

empirical formula	C ₁₈ H ₂₉ ClNO ₂ PRu	C ₁₈ H ₂₉ AlCl ₄ FeNO ₂ P
fw	458.91	547.02
cryst syst	monoclinic	monoclinic
space group	P2 ₁	P2 ₁ /c
unit cell dimens		
<i>a</i> , Å	8.0741(9)	22.468(1)
<i>b</i> , Å	15.139(2)	11.8999(5)
<i>c</i> , Å	9.031(1)	19.4901(8)
β, deg	104.613(2)	91.787(1)
volume, Å ³	1068.2(2)	5208.5(4)
<i>Z</i>	2	8
<i>D</i> _{calc} , Mg/m ⁻³	1.427	1.395
μ(Mo Kα), mm ⁻¹	0.943	1.098
no. of reflns collected	12 706	55 820
no. of ind reflns	5701 [<i>R</i> (int) = 0.0726]	13 426 [<i>R</i> (int) = 0.0413]
no. of data/restraints/params	5701/1/217	13426/0/523
goodness-of-fit on <i>F</i> ²	1.033	1.008
final <i>R</i> indices [<i>I</i> > 2σ(<i>I</i>)]		
<i>R</i> 1	0.0470	0.0410
<i>wR</i> 2	0.1207	0.0898
<i>R</i> indices (all data)		
<i>R</i> 1	0.0495	0.0696
<i>wR</i> 2	0.1243	0.1007
res diff peak and hole, e Å ⁻³	1.693 and -2.098	0.672 and -0.276

Table 6. Crystal Data for Compounds 5 and 6

empirical formula	RuC ₁₈ H ₂₉ AlCl ₄ -NO ₂ PRu	C ₁₈ H ₂₉ AlCl ₄ NO ₂ OsP
fw	592.24	681.37
cryst syst	orthorhombic	orthorhombic
space group	<i>Pnm</i> 2 ₁	<i>Pnm</i> 2 ₁
unit cell dimens		
<i>a</i> , Å	10.6688(6)	10.6783(8)
<i>b</i> , Å	10.2497(6)	10.2353(8)
<i>c</i> , Å	12.1164(7)	12.1246(9)
β, deg		
volume, Å ³	1324.9(1)	1325.2(1)
<i>Z</i>	2	2
<i>D</i> _{calc} , Mg/m ⁻³	1.484	1.708
μ(Mo Kα), mm ⁻¹	1.102	5.322
no. of reflns collected	15234	5322
no. of ind reflns	3588 [<i>R</i> (int) = 0.0225]	2641 [<i>R</i> (int) = 0.0286]
no. of data/restraints/params	3588/1/142	2641/1/142
goodness-of-fit on <i>F</i> ²	1.105	1.058
final <i>R</i> indices [<i>I</i> > 2σ(<i>I</i>)]		
<i>R</i> 1	0.0167	0.0239
<i>wR</i> 2	0.0435	0.0579
<i>R</i> indices (all data)		
<i>R</i> 1	0.0168	0.0239
<i>wR</i> 2	0.0436	0.0586
res diff peak and hole, e Å ⁻³	0.178 and -0.527	0.610 and -0.659

shift and osmium the highest. Other than the presence of two isomers in the iron complex, the infrared spectra show little variation as the metal is changed. The metal to phosphorus distances reflect the metal radii, with a large increase from Fe to Ru, and a further smaller increase from Ru to Os. The P–N distances, which give an indication of the extent of N to P π donation, do not vary significantly between the three complexes.

The spectroscopic and structural parameters of these group 8 aminophosphinidene complexes show the presence of a significant nitrogen to phosphorus donor interaction that serves to stabilize the electron-deficient phosphorus center. The short P–N distance and the planar geometry at nitrogen, along with the high barrier

to rotation about the PN bond, clearly show the presence of this nitrogen to phosphorus donor interaction. Like Fischer-type carbene complexes, the aminophosphinidene complexes are best considered to be formally derived from the singlet state of free phosphinidene, which has two lone pairs and an empty p orbital. One lone pair is donated to the metal center, while the second lone pair remains sterically active, resulting in the trigonal geometry at phosphorus. The empty p orbital is then capable of accepting π-back-donation from the metal or donation from the nitrogen lone pair. It is also worth noting that while Cp* and NⁱPr₂ groups are somewhat bulky, and therefore may provide some steric protection of the phosphinidene–metal bond, it is evident from Figures 4–6 that the phosphorus atom in **3**, **4**, and **5** is not severely encumbered.

Conclusions

We have developed a versatile route to aminophosphinidene complexes involving abstraction of chloride from chlorophosphido complexes and applied it to the formation of group 8 phosphinidene complexes. Heteroatom substitution is an effective way of stabilizing late metal phosphinidene complexes. The stability of the iron phosphinidene complex, previously thought to be thermally unstable, provides further evidence that given appropriate electron donation to the phosphorus center, terminal phosphinidene complexes of first-row transition metals are not fundamentally unstable.

Experimental Section

Preparation of Compounds. General Comments. All procedures were carried out using standard Schlenk techniques or in a glovebox under a nitrogen atmosphere. THF was distilled from Na/benzophenone. Dichloromethane and hexane were purified using solvent purification columns containing alumina (dichloromethane) or alumina and copper catalyst (hexane). Deuterated chloroform was vacuum distilled from P₂O₅. The NMR spectra were recorded at 400 MHz (¹H) or 161.975 (³¹P{¹H}) in CDCl₃, and IR spectra were recorded in CH₂Cl₂ solution. The compounds [Cp*Fe(CO)₂{P(Cl)NⁱPr₂}],¹¹ [Cp*Ru(CO)₂]₂,²⁰ and [Cp*OsH(CO)₂]₂²¹ were synthesized according to published procedures.

a. [Cp*Ru(CO)₂{P(Cl)NⁱPr₂}] (2). [Cp*Ru(CO)₂]₂ (500 mg, 0.855 mmol) and KC₈ (231 mg, 1.71 mmol) were dissolved in 50 mL of THF and stirred for 2 h. The resulting solution was filtered and added to ⁱPr₂NPCl₂ (1 mL, 730 mg, 6.7 mmol) in 50 mL of THF. The solvent was removed in vacuo, and the resulting solid was extracted with 15 mL of hexane, filtered, and cooled to -35 °C for 48 h, resulting in the formation of large yellow crystals. Yield: 375 mg, 48%. IR (ν_{CO}, hexane solution): 2015, 1962 cm⁻¹. ¹H NMR (25 °C): δ 3.98 (vb, 1H, CH(CH₃)₂), 3.69 (vb, 1H, CH(CH₃)₂), 1.95 (s, 15H, C₅(CH₃)₅), 1.30 (vb, 12H, CH₃). ¹H NMR (-60 °C): δ 3.94 (septet, 1H, CH(CH₃)₂, ³J(HH) = 6.3 Hz), 3.54 (septet, 1H, CH(CH₃)₂, ³J(HH) = 6.6 Hz), 1.95 (s, 15H, C₅(CH₃)₅), 1.39 (d, 3H, CH₃, ³J(HH) = 6.6 Hz), 1.25 (d, 3H, CH₃, ³J(HH) = 6.3 Hz), 1.15 (d, 3H, CH₃, ³J(HH) = 6.6 Hz), 1.11 (d, 3H, CH₃, ³J(HH) = 6.3 Hz). ³¹P NMR: δ 341. Anal. Calcd for C₁₈H₂₉O₂PNCIRu: C, 47.11 H 6.37, N 3.05. Found: C, 47.32; H, 6.97; N, 3.23.

b. [Cp*Os(CO)₂{P(Cl)NⁱPr₂}] (3). [Cp*OsH(CO)₂]₂ (110 mg, 0.28 mmol) was dissolved in THF (15 mL). BuLi (0.115 mL,

(20) King, R. B.; Iqbal, M. Z.; King, A. D., Jr. *J. Organomet. Chem.* **1979**, *171*, 53–63.

(21) Hoyano, J. K.; May, C. J.; Graham, W. A. G. *Inorg. Chem.* **1982**, *21*, 3095.

2.5 M in hexane, 0.28 mmol) was added. The resulting solution of $\text{Li}[\text{Cp}^*\text{Os}(\text{CO})_2]$ was then added in small portions over 1 h to ${}^i\text{Pr}_2\text{N}(\text{PCl}_2)_2$ (42 μL , 0.28 mmol) in THF (15 mL). The solvent was removed in vacuo, and the residue was extracted with hexane, filtered, and cooled to $-35\text{ }^\circ\text{C}$ for 48 h, resulting in the formation of pale yellow crystals. Yield: 90 mg, 59%. IR νCO (hexane): 2007 s, 2002 vw, 1952 s, 1941 vw. ${}^1\text{H}$ NMR (25 $^\circ\text{C}$): δ 4.1 (vb, 1H, $\text{CH}(\text{CH}_3)_2$), 3.6 (vb, 1H, $\text{CH}(\text{CH}_3)_2$), 2.06 (s, 15H, $\text{C}_5(\text{CH}_3)_5$), 1.3 (vb, 12H, CH_3). ${}^{31}\text{P}$ NMR: δ 304. Anal. Calcd for $\text{C}_{18}\text{H}_{29}\text{NO}_2\text{PClO}_2$: C, 39.45; H, 5.33; N, 2.56. Found: C, 39.10; H, 5.72; N, 2.54.

c. $[\text{Cp}^*\text{Fe}(\text{CO})_2\{\text{PN}^i\text{Pr}_2\}][\text{AlCl}_4]$ (4). $[\text{Cp}^*\text{Fe}(\text{CO})_2\{\text{P}(\text{Cl})\text{N}^i\text{Pr}_2\}]$ (50 mg, 0.12 mmol) and AlCl_3 (24 mg, 0.18 mmol) were dissolved in 0.5 mL of CH_2Cl_2 , resulting in a color change to darker yellow. Dry hexane was layered on top of the CH_2Cl_2 solution, resulting in gradual formation of yellow crystals of $[\text{Cp}^*\text{Fe}(\text{CO})_2\{\text{PN}^i\text{Pr}_2\}][\text{AlCl}_4]$ (2). Yield: 50 mg, 76%. IR νCO (CH_2Cl_2): 2050, 2036, 2007, 1999 cm^{-1} . ${}^1\text{H}$ NMR: δ 5.04 (septet, 1H, ${}^3J_{\text{HH}} = 6.6$, $\text{CH}(\text{CH}_3)_2$), 4.64 (doublet of septets, 1H, ${}^3J_{\text{HH}} = 6.8$, ${}^3J_{\text{HP}} > 2$, $\text{CH}(\text{CH}_3)_2$), 2.01 (singlet, 15H, $\text{C}_5(\text{CH}_3)_5$), 1.60 (doublet, 6H, ${}^3J_{\text{HH}} = 6.6$, CH_3), 1.49 (doublet, 6H, ${}^3J_{\text{HH}} = 6.8$, CH_3). ${}^{31}\text{P}$ NMR: δ 965. Anal. Calcd for $\text{C}_{18}\text{H}_{29}\text{O}_2\text{PNAICl}_4\text{Fe}$: C, 39.52; H, 5.34; N, 2.56. Found: C, 39.22; H, 5.69; N, 2.56.

d. $[\text{Cp}^*\text{Ru}(\text{CO})_2\{\text{PN}^i\text{Pr}_2\}][\text{AlCl}_4]$ (5). $[\text{Cp}^*\text{Ru}(\text{CO})_2\{\text{P}(\text{Cl})\text{N}^i\text{Pr}_2\}]$ (70 mg, 0.15 mmol) and AlCl_3 (20 mg, 0.15 mmol) were dissolved in 0.5 mL of CH_2Cl_2 . The resulting yellow solution was layered with hexane. Over 7 days, large yellow crystals formed. Yield: 47 mg, 52%. IR νCO (CH_2Cl_2): 2051, 2007 cm^{-1} . ${}^1\text{H}$ NMR: δ 5.06 (septet, 1H, ${}^3J_{\text{HH}} = 6.6$, $\text{CH}(\text{CH}_3)_2$), 4.69 (doublet of septets, 1H, ${}^3J_{\text{HH}} = 6.8$, ${}^3J_{\text{HP}} = 2$, $\text{CH}(\text{CH}_3)_2$), 2.15 (singlet, 15H, $\text{C}_5(\text{CH}_3)_5$), 1.60 (doublet, 6H, ${}^3J_{\text{HH}} = 6.6$, CH_3), 1.51 (doublet, 6H, ${}^3J_{\text{HH}} = 6.8$, CH_3). ${}^{31}\text{P}$ NMR: δ 932. FAB-MS (m/z): 593 $[\text{M} + \text{H}]^+$. Anal. Calcd for $\text{C}_{18}\text{H}_{29}\text{O}_2\text{PNAICl}_4\text{Ru}$: C, 36.50; H, 4.94; N, 2.36. Found: C, 36.18; H, 5.19; N, 2.36.

e. $[\text{Cp}^*\text{Os}(\text{CO})_2\{\text{PN}^i\text{Pr}_2\}][\text{AlCl}_4]$ (6). $[\text{Cp}^*\text{Os}(\text{CO})_2\{\text{P}(\text{Cl})\text{N}^i\text{Pr}_2\}]$ (90 mg, 0.16 mmol) and AlCl_3 (33 mg, 0.24 mmol) were

dissolved in 0.5 mL of CH_2Cl_2 . The resulting yellow solution was layered with hexanes. Over 7 days, pale yellow crystals had formed. Yield: 47 mg, 52%. IR νCO (CH_2Cl_2): 2055, 2005 cm^{-1} . ${}^1\text{H}$ NMR: δ 5.06 (septet, 1H, ${}^3J_{\text{HH}} = 6.6$, $\text{CH}(\text{CH}_3)_2$), 4.67 (doublet of septets, 1H, ${}^3J_{\text{HH}} = 6.7$, ${}^3J_{\text{HP}} = 3$, $\text{CH}(\text{CH}_3)_2$), 1.57 (singlet, 15H, $\text{C}_5(\text{CH}_3)_5$), 1.50 (doublet, 6H, ${}^3J_{\text{HH}} = 6.6$, CH_3), 1.51 (doublet, 6H, ${}^3J_{\text{HH}} = 6.8$, CH_3). ${}^{31}\text{P}$ NMR: δ 838. Anal. Calcd: C, 31.73; H, 4.29; N, 2.06. Found: C, 28.04; H, 4.47; N, 2.09. Satisfactory analyses could not be obtained because the pale yellow crystals could not be completely separated from crystals of AlCl_3 . The molecule was thus characterized by X-ray diffraction studies of a single crystal.

X-ray Data Collection and Structure Solution. Suitable crystals of compounds **2**, **4**, **5**, and **6** were mounted on glass fibers. Diffraction measurements were made on a Siemens SMART CCD automatic diffractometer using graphite-monochromated Mo K α radiation at $-100\text{ }^\circ\text{C}$. The unit cell was determined from randomly selected reflections obtained using the SMART CCD automatic search, center, index, and least-squares routines. Crystal data and collection parameters are listed in Table 2. Integration was carried out using the program SAINT, and an absorption correction was performed using SADABS. Structure solution was carried out using the SHELXTL 5.1 suite of programs. Initial solutions were obtained by direct methods and refined by successive least-squares cycles.

Acknowledgment. This work was supported by the National Research Council of Canada and grants from the Natural Sciences and Engineering Research Council of Canada (to A.J.C.) and an NRC-NSERC Canadian Government Laboratories Visiting Fellowship (to B.T.S.).

Supporting Information Available: Crystallographic data for compounds **2** and **4–6**. This information is available free of charge via the Internet at <http://pubs.acs.org>.

OM030386X